Separation Science and Technology
Publication details, including instructions for authors and subscription information:
http://www.informaworld.com/smpp/title~content=t713708471

Separation of a Two-Component Particulate Material Mixture by a Vibro-Impacting Separator

K. Erdész[a]
[a] RESEARCH INSTITUTE FOR TECHNICAL CHEMISTRY HUNGARIAN ACADEMY OF SCIENCES VESZPRÉM, HUNGARY

To cite this Article Erdész, K.(1984) 'Separation of a Two-Component Particulate Material Mixture by a Vibro-Impacting Separator', Separation Science and Technology, 19: 4, 241 — 259
To link to this Article: DOI: 10.1080/01496398408068581
URL: http://dx.doi.org/10.1080/01496398408068581

SEPARATION SCIENCE AND TECHNOLOGY, 19(4 & 5), pp. 241-259, 1984

Separation of a Two-Component Particulate Material Mixture by a Vibro-Impacting Separator

K. ERDÉSZ

RESEARCH INSTITUTE FOR TECHNICAL CHEMISTRY
HUNGARIAN ACADEMY OF SCIENCES
VESZPRÉM, HUNGARY 8200

Abstract

The vibro-impacting separator, the so-called Paddy table, is widely used for the separation of the components of binary mixtures of particulate materials. This paper presents an improved mathematical model of vibro-impacting separation and experimental results aimed at the further investigation of vibro-impacting motion, the adequacy of the model, and the improvement of the efficiency of vibro-impacting separation, with special attention to friction between the particles and the operational element of the separator. It is concluded that friction decreases the instability of the periodic symmetric motion of the particles and that the model adequately represents the physical system in the range of the operational variables tested. Also, it is found that the formulas obtained are suitable for design purposes and that friction decreases the separation efficiency. In conclusion, we believe that vibro-impacting separation is a promising candidate for many fields of industry.

INTRODUCTION

Separation of particulate mixtures into two or more components according to preset technological requirements is an important task in the chemical, pharmaceutical, food processing, and other industries. Separation might produce a narrow size cut from polydisperse mixtures, it might classify the mixture according to particle size, or it might separate from the mixture the particles which have undesirable technological or other characteristics. These separation goals bear different consequences upon product quality. In

 0149-6395/84/1904-0241$3.50/0

the first two cases the goal is the production of maximized amounts of fractions within given particle size limits. In the latter case the requirements are more severe, for all undesirable particles have to be removed from the mixture as contaminants. Naturally, processed food must not contain harmful (poisonous, hard-to-digest) contituents, nor may pharmaceuticals or chemical intermediates be contaminated with undesirable active or dangerous materials. Therefore, selection of the right separation method requires great care for, apart from economics, feasibility of technological realization also has to be taken into consideration.

When harmful components are to be removed, then the system can be thought of as a binary mixture which contains only useful and harmful components. In this case the polydisperse nature of the mixture is of no importance, except when the particle size of the harmful and useful components differs greatly enough to allow for the removal of the contaminants in a given size fraction. Good results can be obtained when there is no overlap between the particle sizes of the two fractions. More frequently, however, there is no correlation between particle size and harmfulness, i.e., the size distribution of the base material is identical with that of the contaminant. Such contaminants are called hard-to-separate contaminants (*1*). At present, mechanical separation methods are used most frequently for the removal of such hard-to-separate contaminants, for in industrial practice the mechanical characteristics of most materials differ considerably. Such machines are produced on the assembly line. Their price, operation, and maintenance costs are not outrageously excessive and their efficiency is acceptable. The drawback of machines based on the detection of optical or electric characteristics is that their application possibilities are limited to a certain number of materials, and their price and operation costs are high. Their important asset is that each particle is tested for the selected characteristic (e.g., color, electrostatic charge) so, theoretically, "absolute" separation can be achieved, fulfilling even the most exacting demands. Since the productivity of optical separators is low, research should be directed toward the improvement of the separation efficiency of highly productive mechanical separators.

Generally, several particle characteristics simultaneously influence the mechanical separation of particulate mixtures. Therefore, separation efficiency and product purity can both be improved if the design of the operation element of the separator ensures that all beneficial factors come into play and promote separation. Such a system is the vibro-impacting separator, the so-called Paddy table. The results of theoretical and experimental work aimed at the improvement of its separation efficiency are presented in this paper.

LITERATURE OVERVIEW

The operation principles of the Paddy table were described some 100 years ago. However, intensive investigation of its operation principles began only recently (*2*). The operating element of the machine is a zig zag channel (cf. Fig. 1) which consists of geometrically identical sections located along its longitudinal axis. The side walls of the sections are arranged symmetrically, at α degrees, with respect to the main axis. The walls are perpendicular to the bottom of the channel. The channel itself slants at an angle β with respect to the horizontal line. There are several parallel channels in an operational unit. For increased productivity and space economy, the operational units are located above each other and they are joined into multistory structures. There is a cam mechanism in the horizontal plane of the machine frame. This ensures the harmonic oscillating movement of the operation element, perpendicular to its longitudinal (main) axis. This motion has a fairly large amplitude ($A^* = 80$–150 mm) and low frequency ($n^* = 60$–120 min^{-1}). The machine is widely used in mills. However, it can be used in any situation when the resilience and friction characteristics of the particles to be separated differ. It is most advantageous when the particles are of medium size (1–5 mm) and their densities and moisture contents are not too high.

Several investigations have dealt with the separation mechanism of Paddy tables. Their results can be briefly summarized as follows.

(*a*) The mixture to be separated is fed onto the operational element of the machine and experiences a periodic motion during the alternating motion of the operational element. The periodic motion starts and ends when the particles hit the side walls of the channel. Thus, segregation of the particles starts at the feeding point (the middle of the channel), and the two different materials begin their travel, in opposite directions, along the separation channel. This vibro-impacting motion is continued until the two separated materials leave the channel at its opposite ends (*3*).

(*b*) Separation efficiency depends on the shape, density, and moisture content of the particles, as well as on their resilience and friction characteristics (*4, 5*).

(*c*) Based on the particle motion which develops in the operational element of the machine, the separation mechanism can be modeled by the vibro-impacting system. Its theoretical investigation allowed for

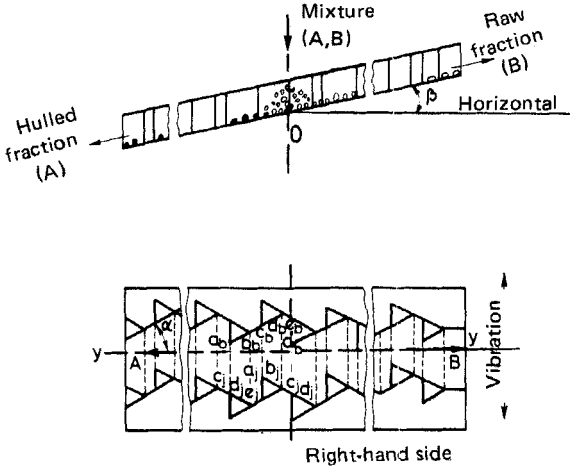

FIG. 1. Operation element of the Paddy table.

generalization of the separation method and a definition of vibro-impacting separation (*6*, *7*).

(*d*) Application of the principles of vibro-impacting separation led to the development of modern high capacity separators which are widely used in the separation technologies of many binary particulate mixtures (*8*).

A shortcoming of the vibro-impacting separation model mentioned is that the effects of friction between the flowing particles and the bottom surface of the channel were not accounted for. Therefore, the model had to be improved.

THE MATHEMATICAL MODEL OF VIBRO-IMPACTING SEPARATION WHICH ACCOUNTS FOR THE EFFECTS OF FRICTION

The model is based on the premise that the individual particles moving in the alternating channel act in a deterministic manner, and also on the simplifying assumption that the particles can be considered as ideal mass centers. The channel is built of successively identical $a_j b_j d_b c_b$ and $c_j d_j b_b a_b$ trapezoid and $b_j c_j e_b d_b$ and $d_j e_j c_b b_b$ parallelogram elements. The directed motion of the material occurs primarily on the slanting side walls of the

trapezoid elements, so it is sufficient to investigate the motion of particles in this part of the operational element. The so-called deterministic model thus obtained is shown in Fig. 2.

The model consists of two major parts. The first constituent is the plane slanting at β degrees with respect to the horizontal, which participates in a harmonic alternating motion in the direction X-perpendicular to the main axis Y. There are impacting walls on this plane which are perpendicular to the plane and are symmetrically located with respect to the main axis at α degrees. The other constituent is a disklike particle model which can freely move on the plane within the impacting walls. This mass center has the physical characteristics of one of the constituents of the material mixture.

The forces acting upon the particle model are gravity G, inertia force P, and friction force F. The plane is located in the X–Y coordinate system in such a manner that the direction of the swinging motion is parallel with axis X, while its main axis is parallel with axis Y.

Motion of the mass center on the alternately moving plane is described by the following differential equation system:

$$m\ddot{x}^* + mgf\cos\beta\frac{\dot{x}^*}{\sqrt{\dot{x}^{*2} + \dot{y}^{*2}}} = mA^*\omega^2\sin(\omega t + \varphi) \qquad (1)$$

$$m\ddot{y}^* + mgf\cos\beta\frac{\dot{y}^*}{\sqrt{\dot{x}^{*2} + \dot{y}^{*2}}} = -mg\sin\beta \qquad (2)$$

Here the inertia force acting upon the particle and the horizontal component of gravity force are at the right-hand side of the equation, and the components of the friction force and the x^* and y^* components of the

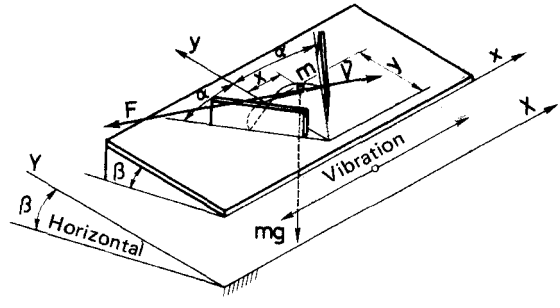

FIG. 2. Model of vibro-impacting separation.

accelerating force acting upon the particle are at the left-hand side of the equation.

The solution of this second-order nonlinear differential equation system requires numerical methods. Also, the initial and boundary conditions cannot be given numerically in advance. Therefore, a computerized solution of the equation, for economic reasons, is out of the question. However, dry friction (Coulomb friction) can be substituted for by viscous drag which is proportional with the velocity. This substitution is justified because the motion of the particles in the channel of the Paddy table is inhibited by the drag of material flow which can be considered viscous.

In this case the motion of the mass center between two impacts can be described by the following linear second-order differential equations:

$$m\ddot{x}^* + K\dot{x}^* = mA^*\omega^2 \sin(\omega t + \varphi) \tag{3}$$

$$m\ddot{x}^* + K\dot{y}^* = -mg \sin\beta \tag{4}$$

To simplify handling, Eqs. (3) and (4) can be rewritten in dimensionless form as

$$\ddot{x} + k\dot{x} = A \sin(\tau + \varphi) \tag{5}$$

$$\ddot{y} + k\dot{y} = -\sin\beta \tag{6}$$

where

$$k = \frac{K}{m\omega}, \qquad A = A^*\frac{\omega^2}{g}, \qquad x = x^*\frac{\omega^2}{g}, \qquad y = y^*\frac{\omega^2}{g},$$

$$\dot{x} = \dot{x}^*\frac{\omega}{g}, \qquad \dot{y} = \dot{y}^*\frac{\omega}{g}, \qquad \ddot{x} = \ddot{x}^*/g, \qquad \ddot{y} = \ddot{y}^*/g$$

In the solution of this differential equation system the primary aim was the generation of the partial solution corresponding to the periodic symmetric motion of the mass center. This can be used as reference in the study of all other possible motion. For the partial solution, one requires the trivial solutions of the differential equations and the algebraic definitions of the initial and boundary conditions which satisfy the periodic symmetric motion at the moment of impact.

The trivial solution of differential Eqs. (5) and (6) are

$$x = C_1 e^{-k\tau} + C_2 - \frac{A}{1+k^2}[k\cos(\tau+\varphi) + \sin(\tau+\varphi)] \tag{7}$$

$$y = C_3 e^{-k} + C_4 - \frac{\sin\beta}{k}\tau \tag{8}$$

Integration constants C_1, C_2, C_3, and C_4 were obtained from the following initial and boundary conditions:

$$\tau = 0, \quad x = x_b, \quad y = y_b$$
$$\dot{x} = \dot{x}_b, \quad \dot{y} = \dot{y}_b, \quad \varphi = \varphi_b \tag{9}$$

$$\tau = n\pi, \quad x = x_j, \quad y = y_j,$$
$$\dot{x} = \dot{x}_j, \quad \dot{y} = \dot{y}_j, \quad \varphi = \varphi_j = \varphi_b + n\pi \tag{10}$$

Subscripts b and j denote the left and right impacting walls, while subscripts 1 and 2 stand for the preimpact and postimpact conditions, respectively.

The symmetry conditions can be obtained from the x and y decomposition of the preimpact velocity vectors, V_1 and V_2, of the particle model (cf. Fig. 3) as follows:

$$x_b = -x_j, \quad y_b = y_j, \quad \dot{x}_{j1} = -\dot{x}_{b1}, \quad \dot{y}_{b1} = \dot{y}_{j1},$$
$$\dot{x}_{j2} = -\dot{x}_{b2}, \quad \dot{y}_{b2} = \dot{y}_{j2} \tag{11}$$

If impact is considered a momentary process, then the energy-dissipation-induced velocity change of impact can be described by the Newtonian and momentary friction hypothesis (9) as follows:

$$R = -\frac{V_2^n}{V_1^n} = -\frac{\dot{x}_{b2} + \dot{y}_{b2}\,\mathrm{tg}\,\alpha}{-\dot{x}_{j1} + \dot{y}_{j1}\,\mathrm{tg}\,\alpha} \tag{12}$$

$$I - \lambda = \frac{V_2^e}{V_1^e} = \frac{-\dot{x}_{b2} + \dot{y}_{b2}\,\mathrm{ctg}\,\alpha}{\dot{x}_{j1} + \dot{y}_{b1}\,\mathrm{ctg}\,\alpha} \tag{13}$$

Here subscripts n and e refer to the normal and tangential vectors as shown in Fig. 3.

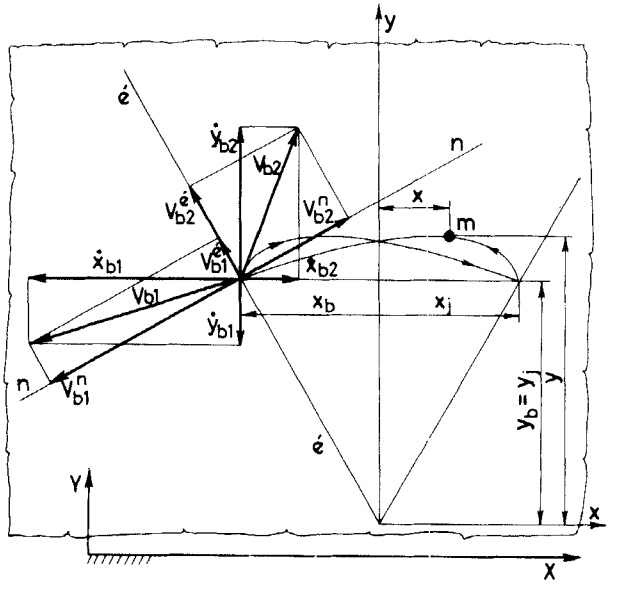

FIG. 3. Decomposition of the impact velocity vectors of the particle.

The integration coefficients are obtained in the following form:

$$C_1 = -\frac{\dot{x}_{b2} - \dot{x}_{b1}}{k(1 + e^{-kn\pi})} \tag{14}$$

$$C_2 = \frac{\dot{x}_{b2} - \dot{x}_{b1}}{2k} \tag{15}$$

$$C_3 = \frac{-\sin\beta\, n\pi}{k(1 - e^{-kn\pi})} \tag{16}$$

$$C_4 = y_b - C_3 = x_b \operatorname{ctg}\alpha - C_3 \tag{17}$$

Integration coefficients C_1, C_2, and C_3 can be substituted into Eqs. (7) and (8), and impact Eqs. (12) and (13) can be used to obtain the partial solutions of the symmetric motion of the particle model for odd ($n = 1, 3, 5, \ldots$) and even ($n = 2, 4, 6, \ldots$) numbered periods as

(*a*) $n = 1, 3, 5, \ldots$:

$$x_b = -\frac{\dot{x}_{b2} - \dot{x}_{b1}}{2k} \operatorname{th} \frac{kn\pi}{2} \pm \frac{A^2}{1+k^2} - \sqrt{\left[\frac{\dot{x}_{b1} + \dot{x}_{b2}e^{-kn\pi}}{1+e^{-kn\pi}}\right]^2} \tag{18}$$

$$\varphi_b = \arccos\left[-\frac{\dot{x}_{b2}e^{-kn\pi} + \dot{x}_{b1}}{\frac{A}{1+k^2}(1+e^{-kn\pi})} \frac{1}{\sqrt{1+k^2}}\right] - \operatorname{arc\,tg}\, k \tag{19}$$

(*b*) $n = 2, 4, 6, \ldots$:

$$x_b = \frac{\dot{x}_{b2} + \dot{x}_{b1}}{2k} \tag{20}$$

$$\varphi_b = \arccos\left[\frac{\dot{x}_{b2}e^{-kn\pi} + \dot{x}_{b1}}{\frac{A}{1+k^2}(1+e^{-kn\pi})} \frac{1}{\sqrt{1+k^2}}\right] - \operatorname{arc\,tg}\, k \tag{21}$$

where in both cases

$$\dot{x}_{b1} = -\sin\beta \frac{[kn\pi e^{-kn\pi} - (1-e^{-kn\pi})][\sin^2\alpha(1+R-\lambda) + \lambda - 1] + kn\pi(1-e^{-kn\pi})}{k(1-e^{-kn\pi})(1+R-\lambda)\sin\alpha\cos\alpha} \tag{22}$$

$$x_{b2} = -\operatorname{tg}\alpha \sin\beta \frac{kn\pi(Re^{-kn\pi} - 1) - (1-e^{-kn\pi})(R+1)}{k(1+e^{-kn\pi})} R\dot{x}_{b1} \tag{23}$$

The velocity components in the direction of y are

$$\dot{y}_{b2} = \sin\beta \frac{kn\pi - (1-e^{-kn\pi})}{k(1-e^{-kn\pi})} \tag{24}$$

$$\dot{y}_{j1} = \sin\beta \frac{kn\pi e^{-kn\pi} - (1-e^{-kn\pi})}{k(1-e^{-kn\pi})} \tag{25}$$

The continuous functions obtained as the result of the calculations are shown in Fig. 7.

EXPERIMENTAL

The purpose of these experiments was to observe the types of motion of vibro-impacting, to check the adequacy of the mathematical model and the actual physical system, and to identify of the effects of friction which influence separation efficiency. The model materials used for the experiments were as follows: Persplex and Bakelite disks of $D = 15$ mm diameter and $V = 10$ mm thickness, treated and untreated rice and millet seed. Specially constructed devices and experimental techniques were used for the determination of the material characteristics R impact coefficient, λ momentary friction coefficient, and f friction coefficient (7). It was shown theoretically that the relationship between viscous drag coefficient K and dry friction coefficient f could not be identified, so a computerized fitting program was used for the determination of the actual value of K (7).

The kinematic scheme of the apparatus used for the examination of vibro-impacting motions and the efficiency of vibro-impacting separations is shown in Fig. 4. The parameters of the apparatus could be continuously adjusted as follows: $A^* = 80$–140 mm, $n = 0$–300 min^{-1}, $\alpha = 20$–$45°$, and $\beta = 1$–$5°$. Particle motion was observed and measured values were checked via the analysis of motion pictures.

The experimental results can be summarized as follows.

Observation of Periodic Symmetric Motion

Having set the experimental parameters (A^*, ω, α, β) and having placed the particle model of given physical characteristics (R, λ, f) into the system, the following motions occurred.

If the initial location of the particle corresponds to the coordinates x_b according to Eq. (18) and $y = x_b \operatorname{ctg} \alpha$, then the particle experiences periodic symmetric motion which is repeated for a few periods. Afterward, due to minor disturbances, the motion soon changes and the particle moves either upward or downward on the slanting plane and leaves it.

If the initial position of the particle is above the previously described coordinates, then no symmetric motion occurs and the particle, hitting the side walls, moves upward.

If the initial position of the particle is below the previously described coordinates, then its resultant motion is directed downward.

The observed motion types of the particle are shown in Fig. 5. When the experiment was repeated with disks of various surface roughness, then it was observed that the rougher the surface (the higher the friction coefficient), the

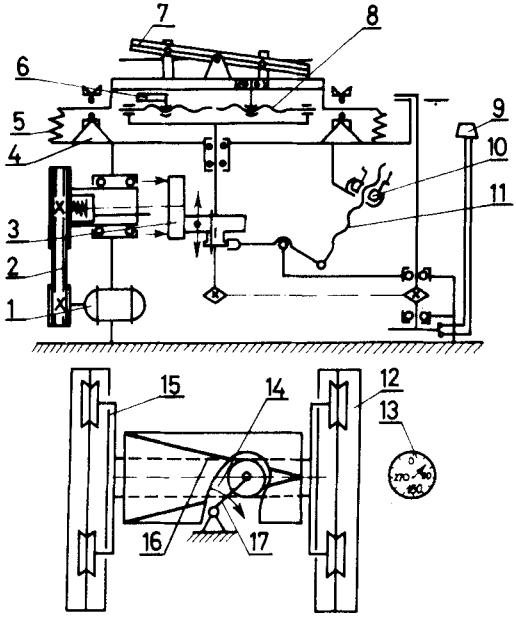

FIG. 4. Kinematic scheme of the apparatus: (1) electric motor, (2) drive belt, (3) friction drive, (4) frame, (5) springs, (6) balance weight, (7) tiltable table, (8) screw spindle, (9) speedometer, (10) handwheel, (11) screw spindle, (12) guide rail, (13) indicator, (14) cam mechanism, (15) carriage, (16) impacting walls, and (17) drive mechanism.

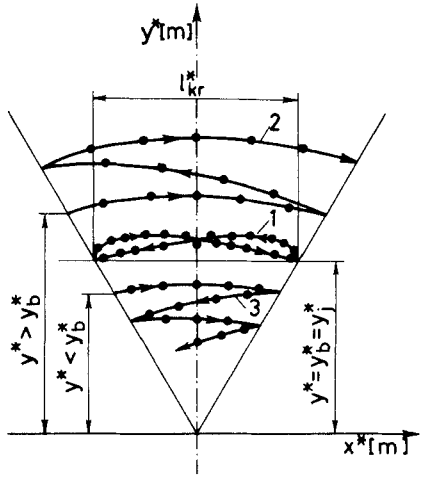

FIG. 5. Motions of the particle model: (1) periodic symmetric motion, (2) resultant upward movement, (3) resultant downward movement.

longer the symmetric periodic motion existed, and the smaller the resultant velocity was.

It was concluded that periodic symmetric motion was not stable in the parameter range tested, and although increasing friction decreased the dynamic instability, it could not fully eliminate it. Gortinskii et al. (*2*) pointed out that the instability of particle motion explained the operation of vibro-impacting separators. If the operational element of the vibro-impacting separator is designed in such a way that the so-called critical coordinates (shown in Fig. 6), which correspond to the physical characteristics of the components of the mixture, are outside of the operational element, then one of the components is below and the other is above their respective critical coordinates and move into opposite directions, i.e., the components become separated.

Checking the Adequacy of the Mathematical Model and the Real Physical System

Comparison of the critical coordinates measured during the experiments with those calculated by Eq. (*18*) indicates that the agreement is good, as shown in Fig. 7. The value of K was determined by fitting the experimental data and formula using computer identification.

In the experiments carried out with particulate materials, the element shown in Fig. 8 was used which corresponded to the trapezoidal section of the operational element of the separator. Since the critical channel cross section corresponding to the critical coordinates at the feeding point $l^* = 2x^*$

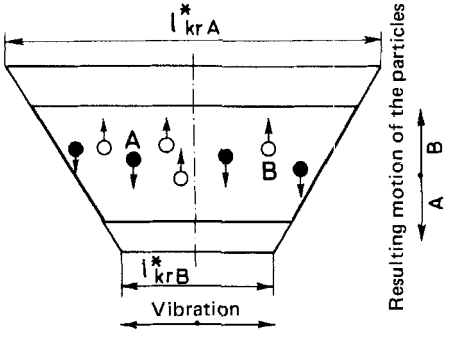

FIG. 6. Schematics of the vibro-impacting separation principle. (●) Physical characteristics of Type A particles: R_A, λ_A, f_A (K_A). (○) Physical characteristics of Type B particles: R_B, λ_B, f_B (K_B).

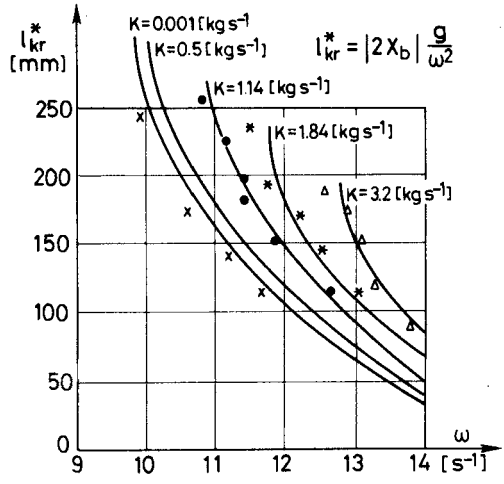

FIG. 7. Changes of the critical size as a function of ω as calculated by Eq. (18). Constant parameters: $A^* = 0.08$ m, $\alpha = 30°$, $\beta = 5°$, $R = 0.46$, $\lambda = 0.9$, (×) $f = 0.22$, (●) $f = 0.31$, (*) $f = 0.36$, (▲) $f = 0.44$.

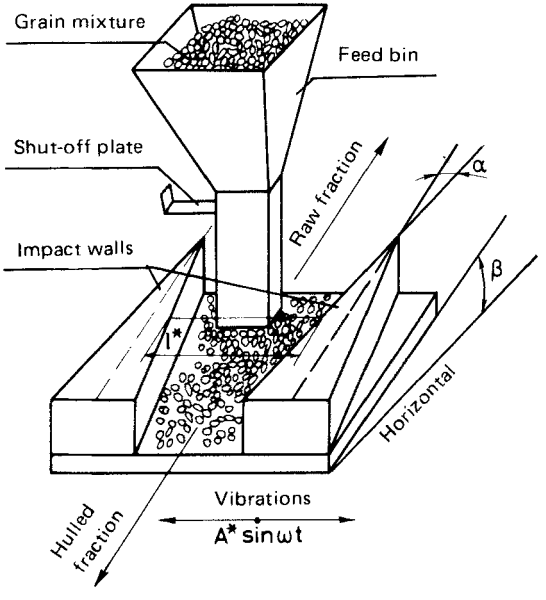

FIG. 8. Schematics of the operation element used for the separation of particulate mixtures.

is constant, the $l^* = 2x^* = f(A^*, \omega, \alpha, \beta, R, \lambda, K)$ function was investigated in an indirect manner. The slope of the base plane was selected as the independent parameter, and ω_{kr} corresponding to the critical size was identified. The indirect measurement is based on the determination of the ratio of the mass flows through the upper and lower edges of the element. At low frequencies the mass flow rate at the lower edge is higher than at the upper edge, while at high frequencies the opposite is true. This means that in the first case the majority of particles in the element is below the critical size, while in the second case the majority is above the critical size. In the case of even distribution, which could be achieved by varying the frequency, the probability of getting particles below and above the critical size at the center line of the trapezoid is identical, i.e., the parameter set used fulfills the $l^* = f(A^*, \omega, \alpha, \beta, R, \lambda, K)$ function.

The parameters used for the experiment were $A^* = 0.08$ m, $l^* = 0.19$ m, $\alpha = 30°$, $\beta = 1$–$5°$, and $\omega = 5$–13 s^{-1}.

Material distribution is characterized by the Q_a/Q_t ratio of the material taken off at the lower edge, Q_a, and the overall amount of material fed in, Q_t. From the distribution curves thus obtained the ω_{kr} and β_{kr} values corresponding to the critical size can be read at $Q_a/Q_t = 50\%$ (cf. Fig. 9). Calculated and measure values are compared in Fig. 10.

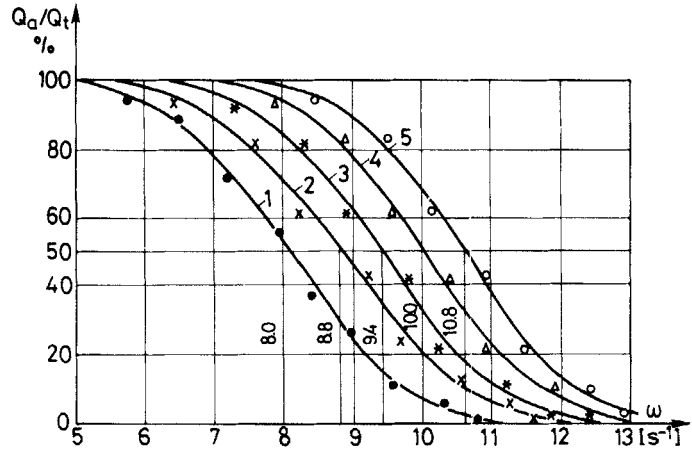

FIG. 9. Distribution curves of the particulate material. Material: Raw millet seed. Constant parameters: $A^* = 0.008$ m, $R = 0.15$, (1) $\beta = 1°$, (2) $\beta = 2°$, (3) $\beta = 3°$, (4) $\beta = 4°$, (5) $\beta = 5°$.

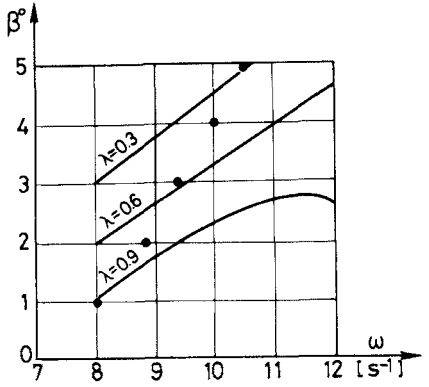

FIG. 10. Comparison of $\beta_{kr} = f(\omega_{kr})$ function and the experimental data.

We conclude that

The mathematical model adequately represents—for all practical purposes—the behavior of particulate material mixtures in the operational element of the vibro-impacting separator.

If the material characteristics are known, then the critical sizes can be calculated by Eq. (18) and can be used for the design of the operational element of vibro-impacting separators.

Examination of the Separation Efficiency of Vibro-Impacting Separator

The effect of friction upon the efficiency of vibro-impacting separation can be studied in experiments carried out with mixtures of raw and processed rice and millet seed.

Separation efficiency can be characterized by both qualitative and quantitative indicators as follows:

$$\eta = \frac{Q_m^a}{Q_m^k} = \frac{\text{mass of separated component in sieve residue}}{\text{mass of component to be separated in the original mixture}} \tag{26}$$

$$\psi = \frac{Q_m^a}{Q_t^a} = \frac{\text{mass of separated component in sieve residue}}{\text{mass of sieve residue}} \tag{27}$$

Since operation of the Paddy table is primarily controlled by the alternation frequency of the operational element, it is convenient to determine the efficiency indicators as functions of this frequency. The effect of friction can be investigated by artifically increasing the friction coefficient between the table and the material mixture. The friction coefficients obtained with various materials and liners are listed in Table 1. It can be seen from Table 1 that the friction coefficients of mixtures are smaller than those of pure materials.

Results of the experiments are shown in Figs. 11 and 12. Curves 1 and 2 were obtained with Liner No. 1 (f_1), and Curves 3 and 4 with Liner No. 2 (f_2). Optimum separation parameters can be obtained from the simultaneous maxima of η and ψ, i.e., at the crossing point of the respective curves. At this point the highest fraction purity is accompanied by the highest yield. It can be seen that in both cases the increasing friction shifts the crossing point toward higher rotation speeds which means that increasing friction decreases the technical efficiency of vibro-impacting separation because, primarily, power consumption is increased. At the same time, as follows from Eq. (18), higher frequencies result in a decrease of the critical channel sizes which fall below the feeding point (or even on the same side of the operation element, but outside of it), resulting in a rapid deterioration or even complete elimination of separation conditions.

An important result of the experiment with respect to the design and operation of vibro-impacting separators is that improved separation efficiency can be achieved by decreasing the friction between the materials to be separated and the structural material of the operating element. Keeping the system clean has the same positive effect.

TABLE 1

Material	Friction coefficient	
	Liner No. 1, f_1	Liner No. 2, f_2
Raw rice	0.65	0.70
Hulled rice	0.71	0.72
Rice, 90% mixture	0.64	0.72
Raw millet seed	0.70	0.80
Hulled millet seed	0.82	0.85
Millet seed, 95% mixture	0.53	0.83

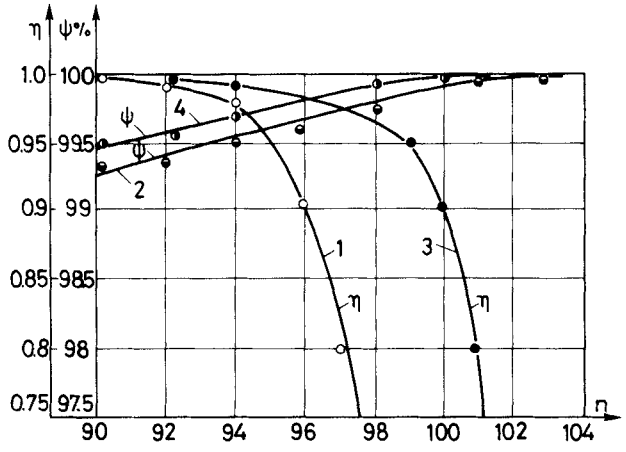

FIG. 11. Optimum parameters of vibro-impacting separation of rice mixture (90% seed, 10% grain mixture): (1, 2) friction coefficient $f = 0.64$, (3, 4) friction coefficient $f = 0.72$.

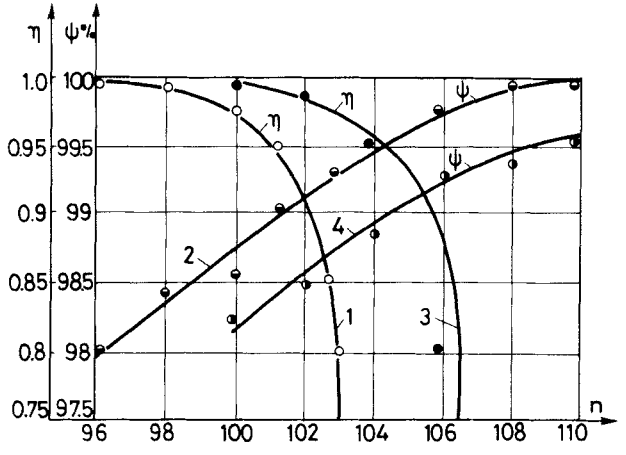

FIG. 12. Optimum parameters of vibro-impacting separation of millet seed mixture (95% seed, 5% grain): (1, 2) friction coefficient $f = 0.53$, (3, 4) friction coefficient $f = 0.83$.

SUMMARY

The results of the theoretical and experimental studies of vibro-impacting separation can be summarized as follows.

The mathematical model of vibro-impacting separation was further developed by accounting for the effects of friction.

It was shown experimentally that increasing friction decreases the dynamic instability of the period symmetric motion of particles, but friction cannot completely eliminate instability, i.e., stable motion cannot be achieved in the parameter range tested.

The mathematical model adequately represents the separation mechanism of particulate mixtures in the operating element of the vibro-impactor. Equation (18) can be used for the design of the operational element if the material characteristics of the mixture are known.

Increasing friction decreases the separation efficiency. This fact has to be reckoned with in the design and operation of vibro-impacting separators.

It is concluded from these result and those published in the literature that vibro-impacting separation is a promising method for the separation of binary particulate mixtures, especially for the removal of hard-to-separate contaminants.

SYMBOLS

A	dimensionless amplitude
A^*	amplitude of vibrations (m)
C_1, C_2, C_3, C_4	integration constants
f	dry friction coefficient
g	gravity constant ($g = 9.81$ m/s)
K	viscous drag coefficient (kg/s)
k	dimensionless viscous drag coefficient
l^*	critical size of the operation element (m)
m	mass of the particle (kg)
n^*	vibration frequency (min^{-1})
Q	mass flow rate (kg/s)
R	impact coefficient
t	time (s)
V_1, V_2	particle velocity before and after impact (m/s)
X^*, Y^*	coordinates of the immobile coordinate system
x^*, y^*	coordinates of the vibrating coordinate system (m)
x, y	dimensionless coordinates of the particle

$\dot{x}, \dot{y}, \ddot{x}, \ddot{y}$	derivative of the dimensionless coordinates
α	angle of impacting walls and the main axis
β	angle of base plane and the horizontal
η	quantitative efficiency
ψ	qualitative efficiency
λ	momentary friction coefficient
τ	dimensionless time
φ	phase angle of impact
ω	circular frequency of vibration (s^{-1})

Acknowledgment

The author is indebted to Dr J. Németh, scientific consultant of the Research Institute for Technical Chemistry of the Hungarian Academy of Sciences, for valuable discussions and comments on this manuscript.

REFERENCES

1. K. V. Drogalin, B. V. Zhigankow, and B. V. Charpow, *Otchiska semian ot trudnootdelimich primesei*, Kolos, Moscow, 1978.
2. V. V. Gortinskii, A. Gemskii, and M. A. Boriskin, *Processii separirovania na zernopererabativaiuschich predpriatiach*, Kolos, Moscow, 1973.
3. I. N. Kupric, *Technologia pererabotki zerna*, Kolos, Moscow, 1972.
4. H. Naumann, *Mühle, 6* (1959).
5. V. V. Gortinski and E. V. Abramow, *Tr., Vses. Nauchno-Issled. Inst. Zerna, 73*, (1972).
6. V. V. Gortinski, E. V. Abramow, and K. Erdész, *Cent. Nauschno-Issled. Inst. Inf. Tekh.-Ekono-mitsch. Issled., 4*, (1978).
7. K. Erdész, Thesis, Moscow, 1978.
8. Soviet Patent Specification BN 15, 573,205, (March 14 1978).
9. A. E. Kobrinski and A. A. Kobrinski, *Vibroudarnije systemi,* Nauka, Moscow, 1973.

Received by editor August 9, 1982
Revised October 3, 1983